

Application News

No. B94

MALDI-TOF Mass Spectrometry

MS Imaging of Rat Liver Tissue Sections Using MALDI-7090

In order to discuss the causes and disease progression, it is important to first clarify the diseased tissue, then determine the quantitative changes and distribution of the molecules present in that diseased tissue. Metabolic analysis by LC-MS or GC-MS is effective in ascertaining quantitative changes in metabolites and lipids, but due to the characteristics of the analytical methods, the information of molecular distribution in the diseased tissue is lost. For this reason, it is difficult to see the changes in molecular distribution associated with the disease progression. In recent study, MS imaging has been utilized as a method to solve this problem. In this article, we introduce an example of the analysis of the molecular dynamics of the disease progression in a non-alcoholic steatohepatitis (NASH) model rat using a combination of MS imaging and LC-MS or GC-MS analysis.

K. Waki

Sample Preparation for MS Imaging

Non-alcoholic steatohepatitis (NASH) is an advanced form of non-alcoholic fatty liver disease (NAFLD), and it may progress to cirrhosis and hepatocellular carcinoma. Quantitative analysis of the biochemical substances in the liver was performed using LC-MS and GC-MS in advance to examine the behavior of the metabolites. In this experiment, we observed the relationship between the pathological findings and molecular distribution using MS imaging with the MALDI-7090 (Fig. 1).

The rats were fed a high-fat diet or normal diet, and freeze-dried tissue sections were prepared from livers removed from rats in the fourth week, the eighth week and the sixteenth week. The prepared liver tissue sections were subjected to pathological staining (azan, HE, sirius red staining) and made into samples for observation of pathological findings. For the samples of MS imaging, stained tissue sections serially taken from high-fat diet group and normal diet group were placed on identical ITO-coated glass slides to allow comparison of the intensity of the signals between these sections.

The matrix (9AA) was deposited on the prepared sample with the iMLayer™ matrix vapor deposition system, then the prepared sample was subjected to measurement after recrystallization.

Visualization of Molecular Distribution in Fibrotic Tissue

The tissue sections of rat liver were stained by azan-staining (Fig. 2, left panel). In Fig. 2, blue parts show fibrotic tissue in liver. Compared to the livers of rats that ingested a normal diet, those of rats with a high-fat diet were observed to have increased fibrotic tissue 8 weeks and 16 weeks after the start of administration (Fig. 2 left; blue parts).

Next, MS imaging with the MALDI-7090 was compared with the azan-stained sections. The target molecules to be imaged were lipids at m/z 833.58 and m/z 788.54, which were chosen from quantitative analytical results of metabolites using LC-MS or GC-MS, and it merged of their two mass images is shown in Fig. 2 right panel. Looking at the distribution of the two target molecules, only m/z 833.58 is present in the liver tissue of rats that ingested a normal diet. On the other hands, the high-fat diet group rat liver shows that the m/z 788.54 is more present in the fibrotic region due to progress from NAFLD to NASH.

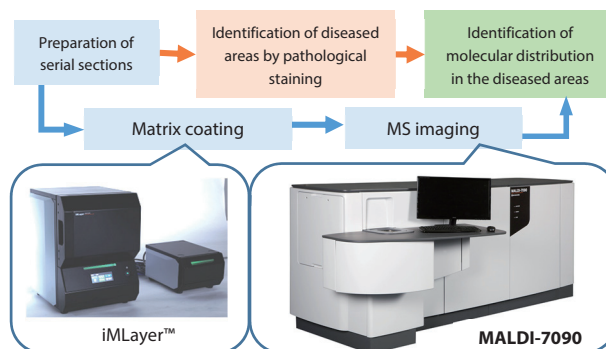


Fig. 1 Workflow of MS Imaging Using the MALDI-7090

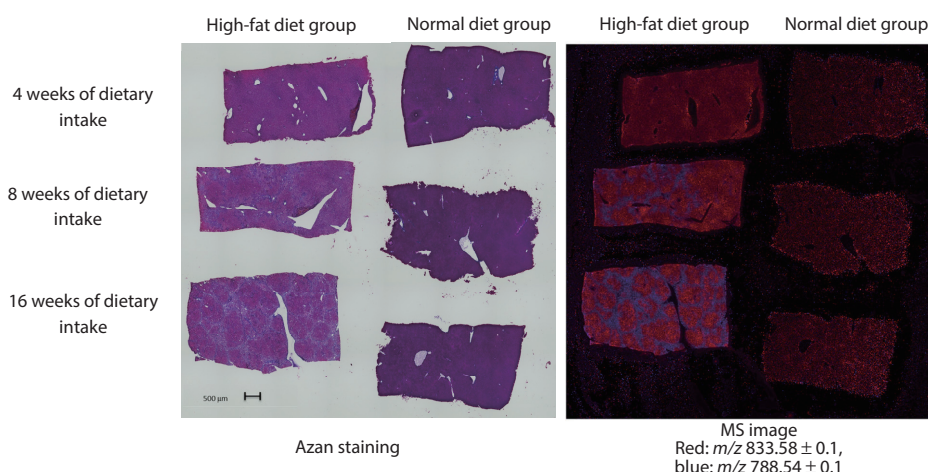


Fig. 2 Differences in Distribution of Target Molecules in Normal Tissues and Diseased Tissues

■ MS Imaging of Bile Acids

The fact that when NAFLD progresses it becomes NASH was mentioned in the description of "Sample Preparation", and up until now the two conditions of NAFLD and NASH have been distinguished by pathological staining. However, observation of optical images with a microscope alone leaves uncertainty in the identification of the condition, and it is difficult to be confident about it as a suitable model in drug development. To solve this problem, in this study MS imaging was performed targeting bile acid that could be expected to fluctuate based on the results of LC-MS or GC-MS (Fig. 3). In the livers of rats that ingested a normal diet, on the right side of Fig. 3, it is found that mainly m/z 498.24 (red), which is primary bile acid, and m/z 514.23 (green) are present. On the other hands, in rats with high-fat diets, the primary bile acid m/z 405.27 (blue) is present in the part where fibrosis progressed.

■ Mathematical Operation with IMAGEREVEAL MS

When the data of the high-fat diet group in Fig. 3 is compared in a time series, there appears to be more m/z 405.27 present in the liver sections after 8 weeks of the high-fat diet than those after 16 weeks of that diet. However, the signal intensity of the mass spectrum obtained varies depending on the condition of the aspect section. For this reason, it may be difficult to compare the raw data or TIC (total ion current) corrected data. The effective course in such cases is to normalize data with respect to another substance and correct the signal intensity to make the comparison.

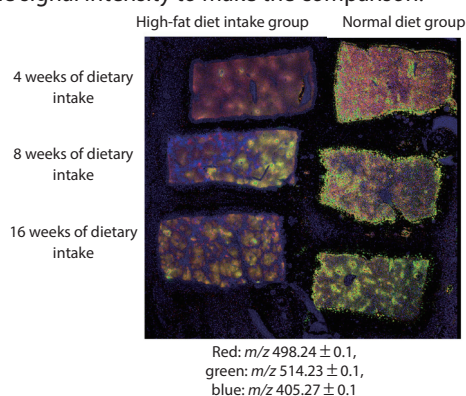


Fig. 3 MS Imaging of Bile Acid

In this case, IMAGEREVEAL MS is useful to analysis. The results of correcting the data obtained in Fig. 3 by using m/z 498.24 and m/z 514.23, which are included in the metabolic pathway of m/z 405.27, are shown on the left in Fig. 4. Comparing these results with the TIC correction image (Fig. 4 right), it was found that there is no great difference in the quantity of m/z 405.27 present after 8 weeks and 16 weeks of high-fat diet intake, in the fibrotic region of NASH model rat livers with high-fat diet intake. In addition, on comparing the m/z 405.27 of NASH model rats that had ingested a high-fat diet for 16 weeks with the same section subjected to hematoxylin-eosin (HE) staining and a serial section subjected to sirius red staining, there was found to be a large quantity of m/z 405.27 in fibrotic tissue (Fig. 5). From these results, it is apparent that there is a large amount of m/z 405.27 in the region where the liver is fibrotic, but that there is little change in the quantity present in correlation to the progress of NASH from the eighth week of high-fat diet intake onward.

Thus, by making use of the advantage that multiple substances can be measured/observed in a single section by MS imaging, and analyzing the obtained data with IMAGEREVEAL MS, MS images that reflected the actual condition of the molecules were obtained, and we were able to understand the relationship between the progress of the pathology and the location of the target molecules more accurately. Further, combining LC-MS and GC-MS data with MS imaging is expected to contribute to the development of new pharmaceuticals through searches for the target molecules of therapeutic drugs for diseases.

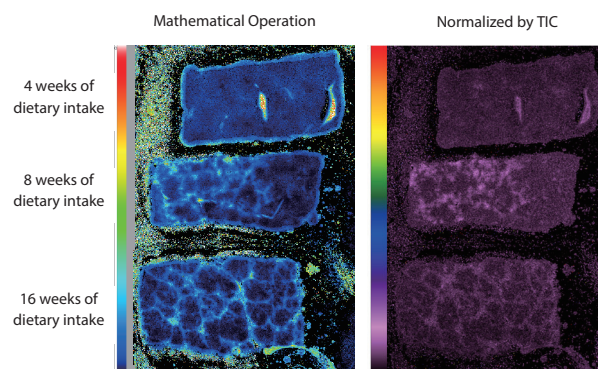


Fig. 4 Mathematical Operation by IMAGEREVEAL MS (m/z 405.27, High-fat Diet Group)

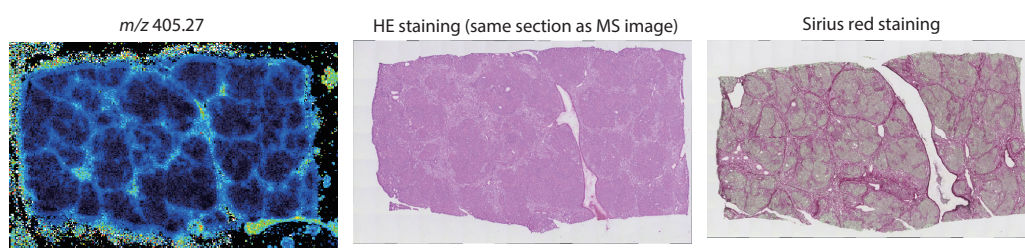


Fig. 5 Comparison of the Distribution of m/z 405.27 and Pathological Staining Results in Rat Liver Tissues after 16 Weeks of a High-fat Diet

Acknowledgments

This report was created as part of a joint research conducted at the Kyushu University Innovation Center for Medical Redox Navigation. We are also grateful to Mr. Makoto Yamazaki of Mitsubishi Tanabe Pharma Co., Ltd. who gave valuable advice along with providing samples.

This product can be used for research purposes only. This has not been approved or certified as a medical device under the Pharmaceutical and Medical Device Act of Japan. It cannot be used for the purpose of medical examination and treatment or related procedures.

iMLayer and IMAGEREVEAL MS are trademarks of Shimadzu Corporation in Japan and/or other countries.

First Edition: Aug. 2019



For Research Use Only. Not for use in diagnostic procedures.

This publication may contain references to products that are not available in your country. Please contact us to check the availability of these products in your country.

The content of this publication shall not be reproduced, altered or sold for any commercial purpose without the written approval of Shimadzu. Shimadzu disclaims any proprietary interest in trademarks and trade names used in this publication other than its own. See <http://www.shimadzu.com/about/trademarks/index.html> for details.

The information contained herein is provided to you "as is" without warranty of any kind including without limitation warranties as to its accuracy or completeness. Shimadzu does not assume any responsibility or liability for any damage, whether direct or indirect, relating to the use of this publication. This publication is based upon the information available to Shimadzu on or before the date of publication, and subject to change without notice.

© Shimadzu Corporation, 2019

Shimadzu Corporation

www.shimadzu.com/an/